doi:10.1093/plphys/kiab290 PLANT PHYSIOLOGY 2021: 187: 2230–2245

Plant Physiology®

Research Article

Transporter SlSWEET15 unloads sucrose from phloem and seed coat for fruit and seed development in tomato

Han-Yu Ko,[1] Li-Hsuan Ho,[1,2] H. Ekkehard Neuhaus [2] and Woei-Jiun Guo [1,*,†]

1 Department of Biotechnology and Bioindustry Sciences, National Cheng Kung University, Tainan 7013, Taiwan
2 Department of Plant Physiology, University of Kaiserslautern, Kaiserslautern, Germany

*Author for communication: wjguo@mail.ncku.edu.tw
†Senior author

H.Y.K. and W.J.G. conceived the project and designed the experiments; H.Y.K. performed most of the experiments and analyzed the data; L.H.H. performed initial expression profiling in fruits. L.H.H. and H.E.N. assisted with yeast uptake experiments; H.Y.K., L.H.H., and W.J.G. wrote the manuscript; H.E.N. edited the manuscript.
The authors responsible for distribution of materials integral to the findings presented in this article in accordance with the policy described in the Instructions for Authors (https://academic.oup.com/plphys/pages/general-instructions) is: Woei-Jiun Guo (wjguo@mail.ncku.edu.tw).

Abstract

Tomato (*Solanum lycopersium*), an important fruit crop worldwide, requires efficient sugar allocation for fruit development. However, molecular mechanisms for sugar import to fruits remain poorly understood. Expression of sugars will eventually be exported transporters (SWEETs) proteins is closely linked to high fructose/glucose ratios in tomato fruits and may be involved in sugar allocation. Here, we discovered that *SlSWEET15* is highly expressed in developing fruits compared to vegetative organs. In situ hybridization and β-glucuronidase fusion analyses revealed SlSWEET15 proteins accumulate in vascular tissues and seed coats, major sites of sucrose unloading in fruits. Localizing SlSWEET15-green fluorescent protein to the plasma membrane supported its putative role in apoplasmic sucrose unloading. The sucrose transport activity of SlSWEET15 was confirmed by complementary growth assays in a yeast (*Saccharomyces cerevisiae*) mutant. Elimination of SlSWEET15 function by clustered regularly interspaced short palindromic repeats (CRISPRs)/CRISPR-associated protein gene editing significantly decreased average sizes and weights of fruits, with severe defects in seed filling and embryo development. Altogether, our studies suggest a role of SlSWEET15 in mediating sucrose efflux from the releasing phloem cells to the fruit apoplasm and subsequent import into storage parenchyma cells during fruit development. Furthermore, SlSWEET15-mediated sucrose efflux is likely required for sucrose unloading from the seed coat to the developing embryo.

Introduction

Tomato (*Solanum lycopersium*) is a key fruit crop worldwide with >$80B annual production value. Development of tomato varieties with high yield and excellent quality have been primary targets for genetic improvement (Ruan et al., 2012; Wang et al., 2019a, 2019b). Photosynthetic assimilation supply is considered a major limiting factor for fruit development (Paul et al., 2018; Quinet et al., 2019). Up to 80% of fruit carbon is imported from source leaves (Hetherington et al., 1998), with sucrose the major form of carbon translocated to tomato fruits (Walker and Ho, 1977; Osorio et al., 2014; Milne et al., 2018). Consequently, increased sucrose

Received February 10, 2021. Accepted June 2, 2021. Advance access publication June 28, 2021

allocation to fruits is a potential strategy to increase yield and quality (Ruan et al., 2012; Osorio et al., 2014).

Tomato fruit development is typically divided into four stages: cell division, expansion, ripening, and maturation (Pesaresi et al., 2014; Quinet et al., 2019). During early-stage cell division, from 0 to 14 d after anthesis (DAA), based on symplastic tracer and radiotracer studies, sucrose is mainly unloaded from sieve element–companion cell (SE-CC) lumens to surrounding vascular parenchyma cells (VPCs) and storage parenchyma cells (SPCs) via connecting plasmodesmata, with a small portion transported via an apoplasmic pathway (Ruan and Patrick, 1995; Patrick and Offler, 1996). However, during rapid expansion (14–40 DAA; Quinet et al., 2019), the young fruit switches to complete apoplastic sucrose unloading from the SE-CCs/VPCs to SPCs (Ruan and Patrick, 1995). Apoplastic sugar transport is indicated by a reduced abundance of plasmodesmata connections between VPCs and SPCs, and loss of mobility of symplasmic dyes in the area of release phloem of tomato pericarp cells (Johnson et al., 1988; Ruan and Patrick, 1995). Apoplasmic unloading of sugars continues for the remaining stages of tomato fruit ripening (Johnson et al., 1988). A feature of the expansion stage is high sugar accumulation, which requires extensive sucrose unloading (Walker and Ho, 1977; Damon et al., 1988; Quinet et al., 2019). This would require a plasma membrane-localized sugar transport mechanism to enable sucrose export from the release phloem to the fruit apoplasm (Lalonde et al., 2003; Osorio et al., 2014; Milne et al., 2018). Involvement of sugar carriers for apoplasmic unloading has been reported in several fruit crops (Braun et al., 2014; Milne et al., 2018), including cucumber (*Cucumis sativus* L.; Hu et al., 2011), apple (*Malus domestica*; Zhang et al., 2004), and grape (*Vitis vinifera* L.; Wang et al., 2003).

However, the molecular carrier responsible for initial sucrose unloading from vascular bundles (SE-CCs or VPCs) to fruit apoplasm has been elusive. Localization in the plasma membrane of SEs in tomato fruits implies that the sucrose transporter LeSUT2 may participate in sugar unloading in fruits (Barker et al., 2000; Hackel et al., 2006). Knockdown of *LeSUT2* expression caused a reduction of 20–40% in both fruit sugar concentration and fruit size (Hackel et al., 2006), whereas overexpression of the pear (*Pyrus bretschneideri*) sugar transporter *Pb*SUT2 in tomato enhanced sucrose concentrations and numbers of fruit produced (Wang et al., 2016). Nevertheless, based on the active transport properties of this symporter (Schulze et al., 2000; Carpaneto et al., 2010; Kuhn and Grof, 2010), *Le*SUT2 likely functions as a retrieval system to prevent sugar loss from SE-CCs instead of exporting sucrose to the fruit apoplast (Hackel et al., 2006; Milne et al., 2018). Passive sugar will eventually be exported transporter (SWEET) uniporters are likely candidate carriers responsible for initial apoplasmic phloem unloading in sink fruits (Osorio et al., 2014; Milne et al., 2018). Latter hypothesis is consistent with the passive transport nature of sucrose unloading in tomato fruit (Ruan and Patrick, 1995; Lalonde et al., 2003).

The *SWEET* gene family has been identified in a wide variety of plants, including tomato (Eom et al., 2015; Feng et al., 2015). Based on their amino acid sequences, SWEET proteins are divided into four distinct clades (Chen, 2013; Eom et al., 2015). Clades I and II mainly transport glucose, Clade III could transport sucrose, and Clade IV can transport fructose. SWEET was first identified as the central player that mediates sucrose efflux from mesophyll cells to the apoplast prior to phloem loading (Chen et al., 2012; Bezrutczyk et al., 2018; Gao et al., 2018). Furthermore, the passive uniporter feature of SWEET members provides an energy-efficient mechanism for unloading sugar in sink organs. In Arabidopsis (*Arabidopsis thaliana*), AtSWEET11, 12, and 15 are localized on plasma membranes of maternal integument and filial endosperm cells to mediate a cascade of sugar unloading that supports embryo development (Chen et al., 2015b). Furthermore, OsSWEET11 and 15 in rice (*Oryza sativa*; Yang et al., 2018), ZmSWEET4c in corn (*Zea mays*; Sosso et al., 2015), and GmSWEET15 in soybean (*Glycine max*; Wang et al., 2019a, 2019b) also participate in apoplasmic sucrose unloading in developing seeds to support endosperm and embryo development. In tomato, based on transient silencing and genetic analyses, SlSWEET1a is also involved in sucrose unloading to sink leaves, as well as regulating the fructose/glucose ratio in ripening fruits (Shammai et al., 2018; Ho et al., 2019). Similarly, expression of pear PuSWEET15 was closely linked with sucrose contents in pear fruit (Li et al., 2020). These findings led us to hypothesize that a *SlSWEET* member expressed in developing tomato fruits is involved in sucrose unloading for fruit development.

In this study, we determined that *SlSWEET15*, belonging to Clade III, was highly expressed during the expansion stage of fruit development. Both *SlSWEET15* RNA and protein were localized in vascular tissues of most fruit tissues. Moreover, SlSWEET15 protein was also present in seed coat and ripening fruits, implicating SlSWEET15 in sugar transport throughout fruit development. Expression in yeast and observations of green fluorescent protein (GFP) fusions demonstrated that SlSWEET15 probably functions as a sucrose-specific transporter on the plasma membrane. Knocking out the SlSWEET15 function by gene-specific editing retarded fruit development and impaired seed filling. In summary, our findings indicate that the SlSWEET15 facilitator has an essential role during fruit and seed development, probably while mediating sucrose unloading from releasing cells.

Results

SlSWEET15 was highly expressed in vascular cells of developing fruits

To identify which *SlSWEET* gene is critical for sugar unloading during fruit expansion, cDNA samples for expression profiling were prepared from immature green tomato fruits

14 DAA. Based on preliminary reverse transcription-quantitative PCR (RT-qPCR) analysis, *SlSWEET15*, which belongs to Clade III *SWEET* members, was strongly expressed during fruit expansion when compared to all other *SlSWEET* genes (Supplemental Figure S1). In expression profiles of Clade III *SlSWEETs* during fruit development (14–42 DAA), *SlSWEET15* had the highest expression in developing green fruits (14–21 DAA), but relatively low expression in mature ripening fruits (35–42 DAA; Figure 1A). Expression of *SlSWEET15* was low in vegetative organs (e.g. roots and leaves) and only weak in fully developed flowers (Figure 1B). Interestingly, during flower development, *SlSWEET15* transcripts substantially increased with maturation of flower buds (6 mm; Figure 1C). Based on these results, we inferred that *SlSWEET15*a might have a specific role during fruit development.

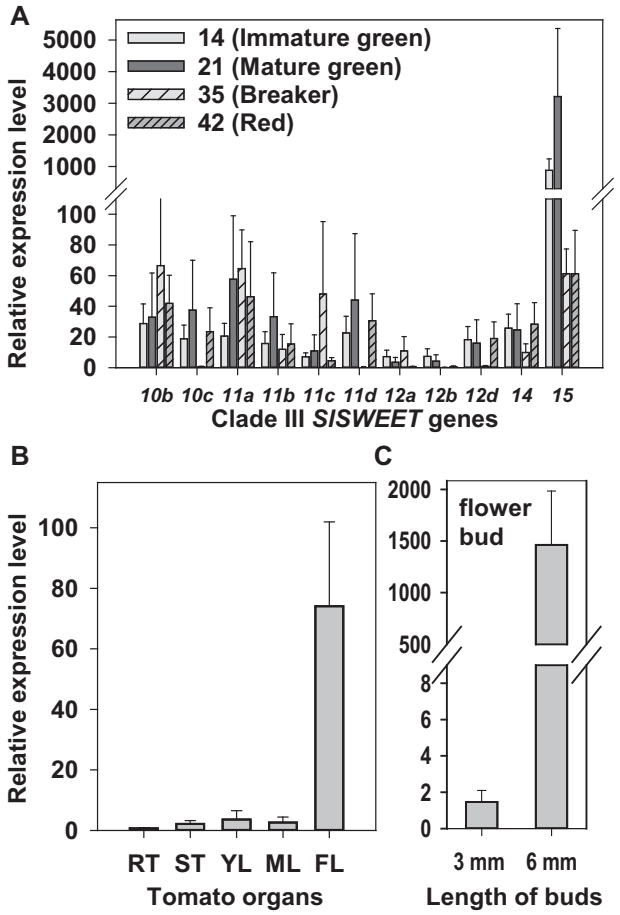

Figure 1 Expression of *SlSWEET15* in tomato organs. A, Expression of representative Clade III *SlSWEET* genes in various stages of tomato fruits. B and C, Expression of *SlSWEET15* in non-fruit organs. Total RNA was isolated from fruits of 14, 21, 35, and 42 DAA (A), or various organs (B), or two sizes of flower buds (C). The derived cDNA was used for RT-qPCR with specific primers. The ordinate is the relative expression level, normalized to the internal control *SlActin7*. Results are mean ± SE from 3 to 7 independent biological repeats. Similar trends had been observed from three independent experiments. RT, root. ST, stem. YL, young leaf. ML, mature leaf. FL: flower.

To address where *SlSWEET15* was expressed, tissue-specific localization of *SlSWEET15* transcripts was examined in mature green fruits (21 DAF) by in situ hybridization with gene-specific fluorescent probes. Due to high similarity between Clade III *SlSWEET* genes, the 3′-UTR (untranslated region) DNA region of *SlSWEET15* was chosen for specific detection (Supplemental Figure S2). To examine possible involvement in sugar unloading, tissue sections containing vascular bundles and seed coats were examined (Supplemental Figure S3A). To identify the possible position of phloem cells, consecutive sections were stained with Aniline blue that detects callose deposits on the sieve plates (Jin et al., 2009). In this case, dotted fluorescing callose suggested the possible location of phloem cells (enlarged details shown in insets, bottom; Figure 2A). In addition, autofluorescence of lignin together with or without distinctively thickened walls implied the cell types of xylem and surrounding VPCs, respectively. When compared to sense probe (Supplemental Figure S3B), clear anti-sense signals were detected in vascular cells of pericarp and columella tissues, including xylem and phloem cells (Figure 2A; Supplemental Figure S3B). In pericarp, weaker signals were also observed in adjunct VPCs and SPCs (Figure 2A). In developing seeds, mRNA signals were additionally detected in seed coats and cells surrounding the embryo (right; Figure 2A; Supplemental Figure S3B). To confirm the specificity of the probe, we also performed alternative in situ hybridization analysis using alkaline phosphatase. Consistently, stronger signals were observed in phloem and neighboring cells residing in pericarp and the columella, as well as in the seed coat (Supplemental Figure S4).

SlSWEET15 proteins accumulated in sugar unloading cells

For several SWEET members, varying ratios of gene expression and protein abundance exist (Guo et al., 2014; Chen et al., 2015a). To examine protein expression, we generated transgenic tomato plants expressing SlSWEET15–β-glucuronidase (GUS) fusion proteins that were derived from the full *SlSWEET15* genomic DNA sequence under control of its native promoter. In T1 transgenic plants, SlSWEET15–GUS fusion proteins were in very low abundance in roots, leaves, or developing flower buds (Figure 2, B–D). In mature flower buds and open flowers, however, histochemical staining readily detected GUS fusion proteins in pollens (Figure 2, D–F). In young developing fruits (14–21 DAA), SlSWEET15-GUS protein was highly abundant in seeds (Figure 2, G–H). When fruits reached mature green (21 DAA), moderate amounts of GUS fusions were observed in vascular tissues of pericarp and columella (arrowheads in Figure 2H), demonstrating a radial dotted pattern in horizontal fruit sections (Figure 2I; Ariizumi et al., 2011). The localization in radial vascular bundles could also be seen in fruit core (left, Supplemental Figure S5). During fruit maturation (35–42 DAA), in addition to seeds and vascular tissues, GUS

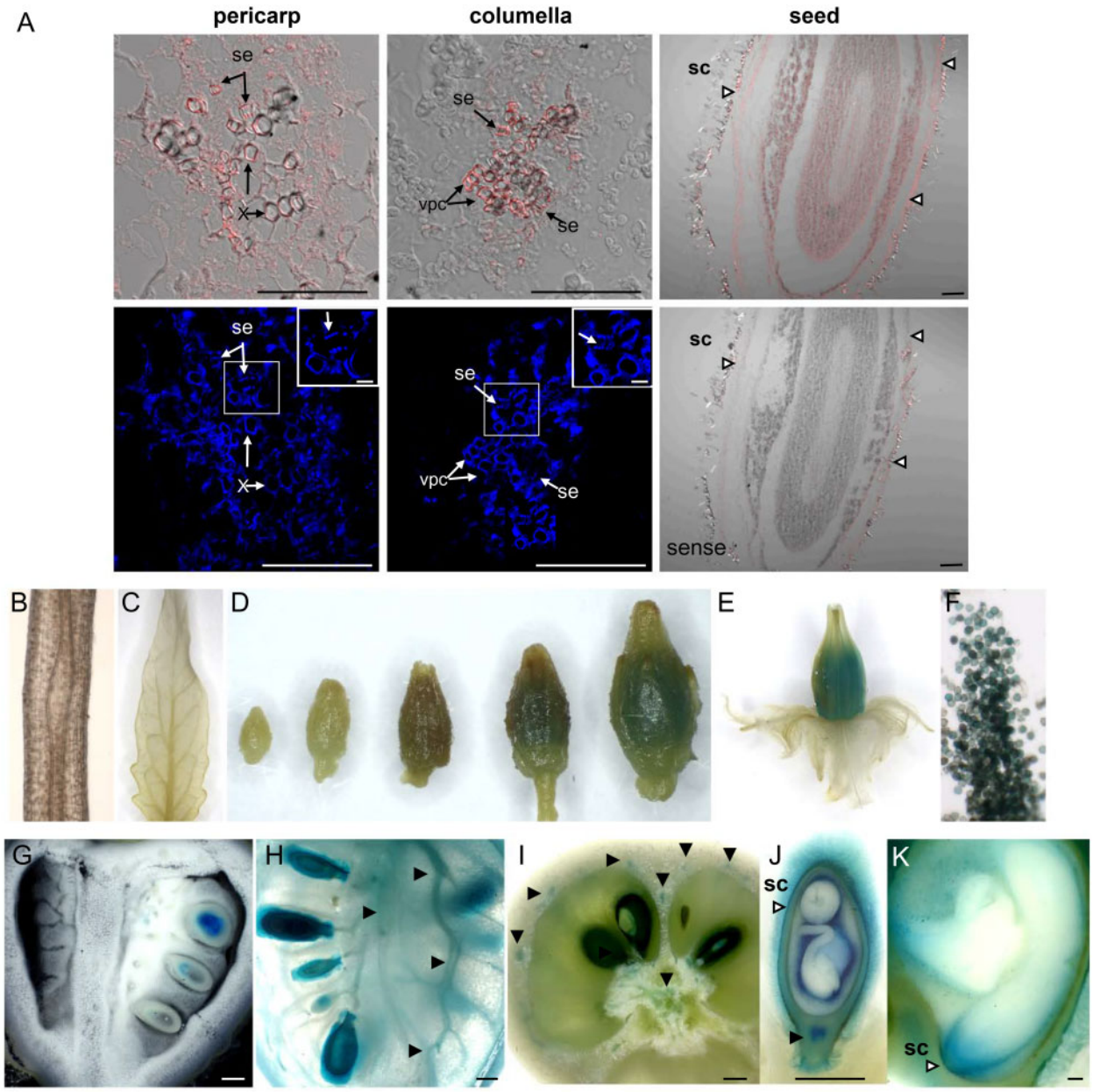

Figure 2 Organ-specific expression pattern of SlSWEET15 in tomato. A, Cell-specific localization of *SlSWEET15* transcripts analyzed by in situ hybridization. Cross-sections of tomato fruits (21 DAA) were hybridized with *SlSWEET15*-specific anti-sense probes. The merged images of bright field and fluorescent signals were shown (top). The consecutive sections of fruit tissues (bottom) were stained with Aniline Blue to detect callose. The dotted fluorescent callose and smooth autofluorescence from the lignified walls suggested the possible cell types of SEs and vascular cells. Enlarged details were shown in insets. For seeds, the section hybridized with a sense probe was shown below. Representative pictures were derived from two independent experiments, containing at least three biological sections. B–J, Histochemical staining of GUS activities in transgenic tomato plants expressing SlSWEET15–GUS fusion proteins driven by *SlSWEET15* native promoter. B, mature roots. C, young leaflet. D, flower buds. E, mature flower. F, pollens. G–H, fruits of 14 and 21 DAA. I, A horizontal section of (H). J, seed. K, zoom-in image of seed. Black and white arrowheads indicate localization of signals in vascular tissues and seed coats, respectively. Representative pictures were derived from three independent experiments, containing at least three biological samples. x, xylem. sc, seed coat. Bars = 100 μm in A, B, F, and K; 1 mm in (C–E) and (G–J); 10 μm for the insets in (A).

activity was also detected in all pericarp cells (Supplemental Figure S5). When developing seeds were hand-sectioned, strong staining signals were observed in seed coat and funiculus vascular tissues (Figure 2, J and K). Substantial accumulation of the GUS fusion protein in vascular tissues and seed coats strongly implicated the SlSWEET15 transporter in sugar unloading in fruits and during seed development.

Dual targeting SlSWEET15 to the plasma membrane and the vacuolar membrane

To examine how SlSWEET15 may participate in sugar transport, subcellular localization of C-terminal translational GFP fusions of SlSWEET15 (SlSWEET15-GFP) was examined in Arabidopsis protoplasts. Fluorescence signals derived from SlSWEET15–GFP fusion lining outside chloroplasts (red autofluorescence, asterisks in Figure 3A) suggests localization of SlSWEET15 at the plasma membrane. Consistently, when co-transformed with the plasma membrane marker plasma membrane intrinsic protein 2A-red fluorescent protein (AtPIP2A-RFP; Nelson et al., 2007), green fluorescence signals derived from SlSWEET15–GFP fusion overlapped with red fluorescence derived from AtPIP2A–RFP fusions (Figure 3B). When cells were lysed, red signals from the plasma membrane marker, AtPIP2A-RFP, were greatly reduced (Supplemental Figure S6A). However, green fluorescence was still observed in a cell internal structure, likely to be the vacuolar membrane. To examine this possibility, the vacuolar membrane marker tonoplast intrinsic protein-red fluorescent protein (AtγTIP-RFP; Jauh et al., 1999) was co-transformed with SlSWEET15-GFP. Consistently, in lysed protoplasts, green fluorescence colocalized with red signals derived from the AtγTIP–RFP fusion on the tonoplast (Supplemental Figure S6B). To further examine localization in vivo, transient expression of SlSWEET15–GFP fusions in *Nicotiana benthamiana* epidermal cells was performed. Green fluorescence was clearly observed on the plasma membrane, lining outside of the nucleus, indicated by no autofluorescence (enlarged details shown in insets, Figure 3C). Interestingly, when cells were under plasmolysis, we observed in addition to plasma membrane a GFP signal at the vacuolar membrane (tonoplast; Supplemental Figure S6C), as indicated by no noticeable Hechtian strands (Speth et al., 2009). Latter results suggest that SlSWEET15 proteins probably mediate sugar transport function on the plasma

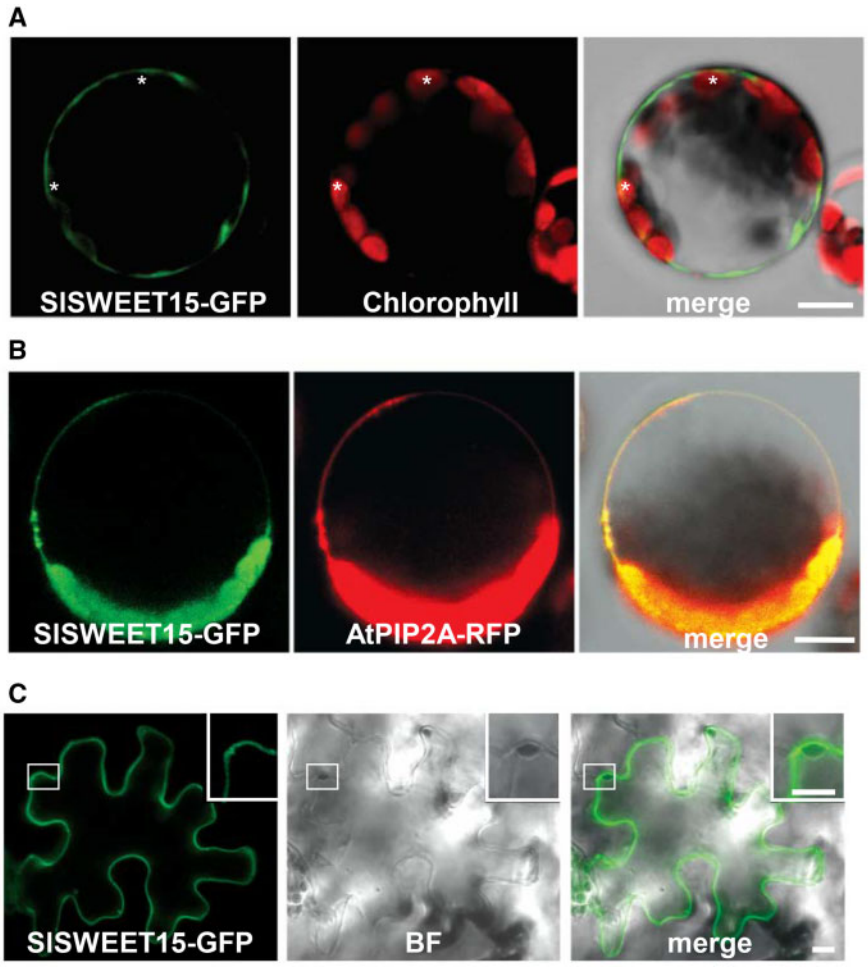

Figure 3 SlSWEET15 localized on the plasma membrane in leaf cells. A, Green fluorescence in Arabidopsis protoplast expressing SlSWEET15–GFP fusion proteins. Asterisks indicate chloroplast autofluorescence (red), lining inside of the plasma membrane. B, Green and red fluorescence were shown in Arabidopsis protoplasts expressing SlSWEET15–GFP fusion proteins and AtPIP2A–RFP fusions, indicating localization to the plasma membrane. C, Confocal images of *N. benthamiana* epidermal leaf cells transiently expressing SlSWEET15–GFP fusions. Enlarged details were shown in insets. All images are single focal planes. Representative pictures were derived from three independent experiments, containing at least three biological samples. Bar = 10 μm.

membrane in tomato developing fruit cells. While during fruit maturation or senescing, SlSWEET15 probably also function on the tonoplast.

Transport activity of SlSWEET15

When comparing amino acid sequence similarity, tomato SlSWEET15 had high identity (up to 50%) to the Arabidopsis homolog AtSWEET15 (Supplemental Figure S7), a sucrose transporter (Chen et al., 2012). To examine transport activity, *SlSWEET15* was expressed in the baker's yeast (*Saccharomyces cerevisiae*) mutant YSL2-1, which lacks all endogenous hexose transporters and the extracellular invertase (Chen et al., 2015a). Accordingly, this mutant yeast showed no or slow growth on medium containing hexoses or sucrose, respectively (Ho et al., 2021). Expression of the Arabidopsis sucrose transporter, *At*SUC2, or yeast hexose transporter, *Sc*HXT5, restored growth on sucrose and hexose-containing medium, respectively (Figure 4A; Supplemental Figure S8). *SlSWEET15* slightly complemented the growth deficiency of YSL2-1, with larger colonies on media containing 2%–5% sucrose (Figure 4A). Consistently, yeast cells expressing *SlSWEET15* grew faster than cells solely expressing the empty vector during the log phase (Figure 4B). The default growth of control YSL2-1 cells expressing the empty vector was probably due to background uptake of sucrose via operation of unknown native sucrose accepting sugar transporters in this mutant (Marques et al., 2017). The low transport activity detected is consistent with the dominant localization of SlSWEET15 in yeast vacuoles, as detected by GFP fusions (Figure 4C). The detection difficulty in yeast cells is in line with the fact that localization of a sugar transporter to the tonoplast would prevent sugar import activity in this recombinant cell system (Chen et al., 2015a). It is thus very likely that the yeast growth observed is mainly due to localization of some SlSWEET15–GFP fusion proteins on the plasma membrane. Conversely, no yeast growth was present on glucose, fructose, or galactose-containing medium (Supplemental Figure S8), implying that SlSWEET15 probably functioned as a sucrose-specific membrane transporter.

Establishment of SlSWEET15 mutants using gene editing

To provide genetic evidence of SlSWEET15 function during fruit development, the clustered regularly interspaced short palindromic repeats (CRISPRs) and CRISPR-associated protein 9 (Cas9) gene-editing strategy was used to generate knockout (KO) mutants (Brooks et al., 2014). The plasmid was designed to produce two guide RNAs (T1 and T2-gRNAs), that would target +266 and +323 positions in exon 3 of *SlSWEET15*, with potential for a substantial deletion (red triangles in Figure 5A; sequences in Supplemental Table S1; Brooks et al., 2014). To screen for editing mutations, we performed PCR on 15 individual T0 transgenic plants (Cas-15-1 to -19) using primers flanking both gRNA targets (Figure 5A, P1 and P2; sequences in Supplemental Table S1). Lines 5 and 12 were identified as potentially having distinct deletions (Supplemental Figure S9A). Detailed DNA sequencing of all PCR products confirmed that Cas-15-5, Cas-15-12, and Cas-15-14 were bi-allelic mutants, whereas Cas-15-6, Cas-15-7, and Cas-15-11 were heterozygous (Hetero) mutants (Figure 5B). Mutations included deletions and point mutations (Figure 5B). The Cas9 gene was detected in all mutant lines (the lower band in Supplemental Figure S9A). Nonmutated transgenic plants that contained the transgene vector (denoted –V, e.g.

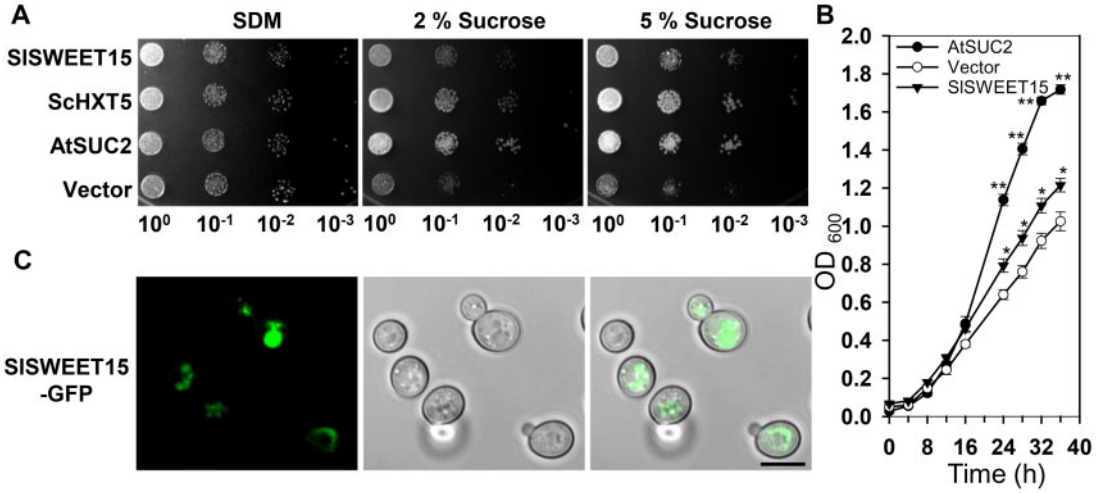

Figure 4 Sucrose transport activity of SlSWEET15 in yeast. A, Growth assay of YSL2-1 cells expressing *Sl*SWEET15. Yeast cells expressing SlSWEET15, ScHXT5, AtSUC2, or an empty vector (vector) were serially diluted (10-fold) and cultured on solid media supplemented with maltose or 2%–5% w/v sucrose, respectively. Images were captured after incubation at 30°C for 4 d. B, Growth curve of yeast cells in (A). Fresh cells were diluted in liquid media supplement with 5% w/v sucrose. OD_{600} of cell cultures were measured every 4 h. Results are mean ± SE from four independent colonies from four independent experiments. Differences from cells containing an empty vector (Student's *t* test): $^{*}P < 0.05$, $^{**}P < 0.01$. C, Vacuolar localization of SlSWEET15–GFP fusions in YSL2-1 yeast cells observed by confocal microscopy. Scale = 5 mm. Representative pictures in (A) and (C) were derived from three independent experiments, containing two independent colonies.

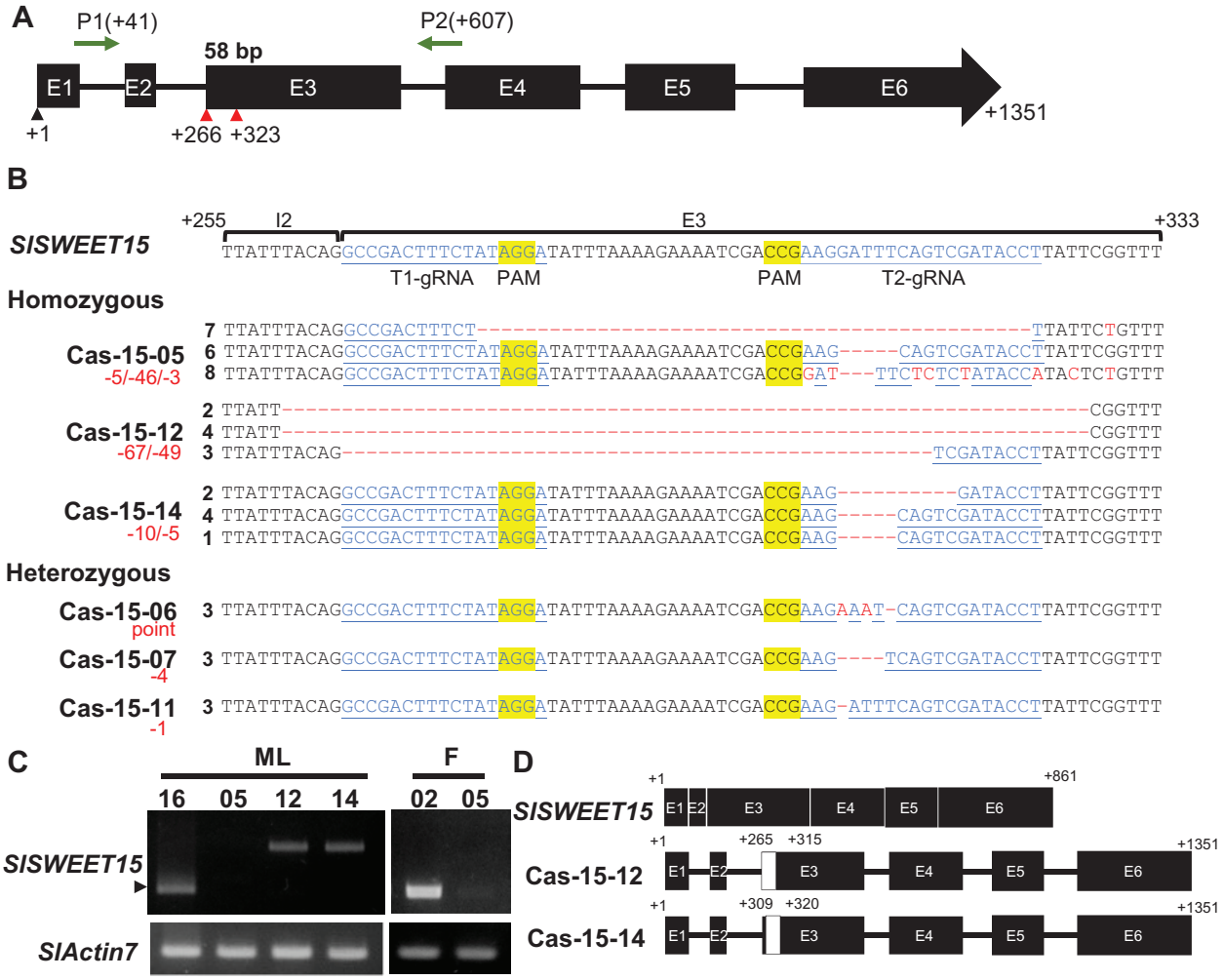

Figure 5 Genotypes of stable *slsweet15* mutant lines via CRISPR/Cas9 gene editing. A, Genomic structure of *SlSWEET15*. P1 and P2 indicated primers used to examine mutation types. Red triangles represented positions of two sgRNA sequences used in the binary vector. All numbers denoted the position of the first sequence relative to the start codon. Boxes and lines indicated regions of exons and introns, respectively. B, Mutation types of *SlSWEET15* DNA in transgenic plants. Genomic DNA was isolated from MLs of T0 transgenic plants (Cas-15-x) and used to amplify gene fragments flanked with P1 and P2 primer in (A). Sequences of three resulting products from each line are shown. Sequences in blue and yellow represented T1/T2 gRNA and PAM sequences, respectively. Red dash lines and font indicated deletion and point mutation, respectively. Numbers in red highlighted mutation types. E, exons. I, introns. C, Expression of *SlSWEET15* in Homo mutants in (B). Total RNA was isolated from MLs or 14-DAA fruit (F) of T0 transgenic plants. Gel pictures of PCR products derived from full-length *SlSWEET15* cDNA and the loading control, *SlActin7*, were shown. Arrowhead indicated the size of WT *SlSWEET15* transcript. D, Schematics of mutation transcripts derived from Homo mutants, Cas-15-5 and Cas-15-12, compared to the WT *SlSWEET15* transcript. White box and numbers indicated the deletion region and position from the ATG in the transcript.

Cas-15-1-V) or lacked the transgenes (denoted – wild-type [WT], e.g. Cas-15-2-WT and Cas-15-16-WT) were used as control plants for growth comparisons.

To confirm expression levels in T0 homozygous (Homo) mutants, full-length of *SlSWEET15* transcripts were examined using mRNA extracted from mature leaves (MLs). In a control plant (Cas-15-16-WT), transcripts of 934 bp were detected (arrowhead in Figure 5C). No transcripts were detected in the Cas-15-5 mutant and the same result was obtained when using mRNA extracted from a 21-DAA fruit (F in Figure 5C). In contrast, larger transcripts (~1,400 bp) were detected in Cas-15-12 and Cas-15-14 mutant lines. Detailed DNA sequencing of PCR products revealed abnormal *SlSWEET15* transcripts. No splicing of all introns occurred in both mutant lines, Cas-15-12 and Cas-15-14, and resulted in nonfunctional proteins (Figure 5D). These results confirmed that Cas-15-5, Cas-15-12, and Cas-15-14 were KO mutants for *SlSWEET15*.

Loss of SlSWEET15 function inhibited fruit and seed development

There were no consistent growth differences in plant size and fruit numbers between T0 mutated transgenic tomato plants (Cas-15-5, Cas-15-12, and Cas-15-14) and WT plants (Supplemental Figure S9B; Supplemental Table S2). However, mature red fruits derived from three independent Homo

KO lines were smaller in size (polar and equatorial lengths; Figure 6A) and fresh weight (~40%; Figure 6B; Supplemental Table S2). In contrast, no differences in fruit size and weight were observed between WT and Hetero plants (Figure 6A and B; Supplemental Table S2). In addition, most seeds derived from Homo KO fruits had suppressed development (Supplemental Figure S9C). The few seeds that did develop were smaller and flaky compared to those from nonmutated plants (-WT/-V; Figure 6C). Consequently, seed weights of KO mutant plants greatly decreased by 90% (Figure 6D; Supplemental Table S2). The embryo and cotyledons had not developed in the mutant seeds (Cas-15-12 and Cas-15-5) compared to nonmutated seeds (Cas-15-1-V), where a well-developed embryo was enclosed by a thin layer of endosperm and seed coat (Figure 6E; Supplemental Figure S9D). These T1 flaky seeds were unable to germinate even when supplied with sugars (Supplemental Figure S9E). Unfortunately, no further phenotypes can be examined in T1 Homo transgenic plants. Interestingly, Hetero mutant plants also had the same seed defects, but less severe, as those in Homo plants (Figure 6, C and D). Some bigger T1 seeds from Hetero lines were viable and could be germinated (Cas-15-6 in Supplemental Figure S9E). These results suggest that SlSWEET15 likely must form a homotrimeric complex to be functional, as reported for a rice OsSWEET (Tao et al., 2015; Gao et al., 2018).

Discussion

SlSWEET15 was involved in vascular sugar transport during fruit development

In tomato fruits, sugars are critical for fruit yield and quality (Pesaresi et al., 2014; Quinet et al., 2019). In particular, once reaching the rapid fruit growth stage, high sugar concentrations will quickly accumulate in pericarp, generating turgor pressure required for fruit expansion (Obiadalla-Ali et al., 2004; Quinet et al., 2019). During tomato fruit development, the cellular pathway of sucrose efflux from the releasing phloem SE-CCs switches from a symplasmic pathway to a complete apoplasmic pathway (Ruan and Patrick, 1995; Patrick, 1997). Accordingly, a plasma membrane sucrose carrier in vascular unloading cells is required, yet still elusive. In this study, we revealed that SlSWEET15 was the possible candidate sucrose carrier to mediate initial sucrose unloading for fruit expansion and seed filling in tomato.

Within all *SlSWEET* members, *SlSWEET15* transcripts were the major isoform highly expressed in fruits that undergo expansion (Figure 1; Supplemental Figure S1). In situ hybridization analysis suggested that during fruit expansion, the *SlSWEET15* transcripts probably accumulated in releasing phloem units, namely the SE-CC complexes and VPCs of major fruit tissues, for example, pericarp and columella (Figure 2A; Supplemental Figures S3 and S4). The pericarp is composed of layers of large, highly vacuolated parenchymatic cells (Czerednik et al., 2012), where sugars largely accumulate for cell expansion. The pericarp accounts for ~50% of the fruit fresh weight at the expansion phase (Gillaspy et al., 1993; Obiadalla-Ali et al., 2004), making a substantial sugar influx mandatory for controlled fruit development. The vascular bundles of fruit columella represent the primary structure connecting the whole-plant vascular system and are the first location in fruits where sugars are unloaded from long-distance allocation (Gillaspy et al., 1993; Baxter et al., 2005). Sucrose and starch consistently accumulate in columella cells during fruit expansion (Baxter et al., 2005; Lemaire-Chamley et al., 2019). Thus, accumulation of *SlSWEET15* transcripts in vascular cells of sugar accumulating fruit tissues was closely associated with increased sugar import activity during the fruit expansion stage, which is almost twice as much as present during fruit maturation (Walker and Ho, 1977). In sum, close association between gene expression and sugar accumulation implicated SlSWEET15 in sugar transport in vascular cells during fruit expansion.

SlSWEET15 may mediate apoplasmic sucrose unloading from fruit vasculature

The role of SlSWEET15 in vascular cells was supported by specific accumulation of SlSWEET15 proteins in vascular bundles of tomato fruits, based on a whole-gene SlSWEET15–GUS translational fusion (Figure 2, B–I; Supplemental Figure S5). Additionally, co-localization of SlSWEET15–GFP fusion proteins with plasma membrane (Figure 3) revealed that SlSWEET15 functioned on the plasma membrane, the major site catalyzing apoplasmic sugar transport (Osorio et al., 2014; Milne et al., 2018). Localization of SlSWEET15 on the plasma membrane was consistent with subcellular localization of other SWEET15 homologs, for example, Arabidopsis AtSWEET15 (Chen et al., 2015b) and pear PuSWEET15 (Li et al., 2020), as well as other Clade III SWEET members involved in sucrose loading in source leaves (Chen et al., 2010, 2012). Most importantly, the constant accumulation of SlSWEET15 proteins after 21 DAA in fruits was fully consistent with the transition timeframe of sucrose unloading from a symplasmic route in fruits at 13–14 DAA to a complete apoplasmic route at 23–25 DAA (Johnson et al., 1988; Ruan and Patrick, 1995; Patrick, 1997). Such apoplasmic sugar unloading from vascular cells also persists throughout fruit maturation (Johnson et al., 1988).

The sucrose-specific transport activity of SlSWEET15, demonstrated by a yeast growth assay (Figure 4), supported its role in sucrose unloading. Low sucrose transport activity of SlSWEET15 proteins was detected due to dominant localization in yeast vacuoles (Figure 4C). Nevertheless, corresponding sucrose transport activity has been generally observed in almost all Clade III SWEET transporters characterized, for example, Arabidopsis AtSWEET10-15 (Chen et al., 2012), cotton (*Gossypium hirsutum*) GhSWEET10 (Cox et al., 2017), pear PuSWEET15 (Li et al., 2020), Cassava (*Manihot esculenta*) MeSWEET10 (Cohn et al., 2014), and rice OsSWEET11 and 15 (Yang et al., 2018), corn ZmSWEET13 (Bezrutczyk et al., 2018). Furthermore, based on genetic evidence, sucrose

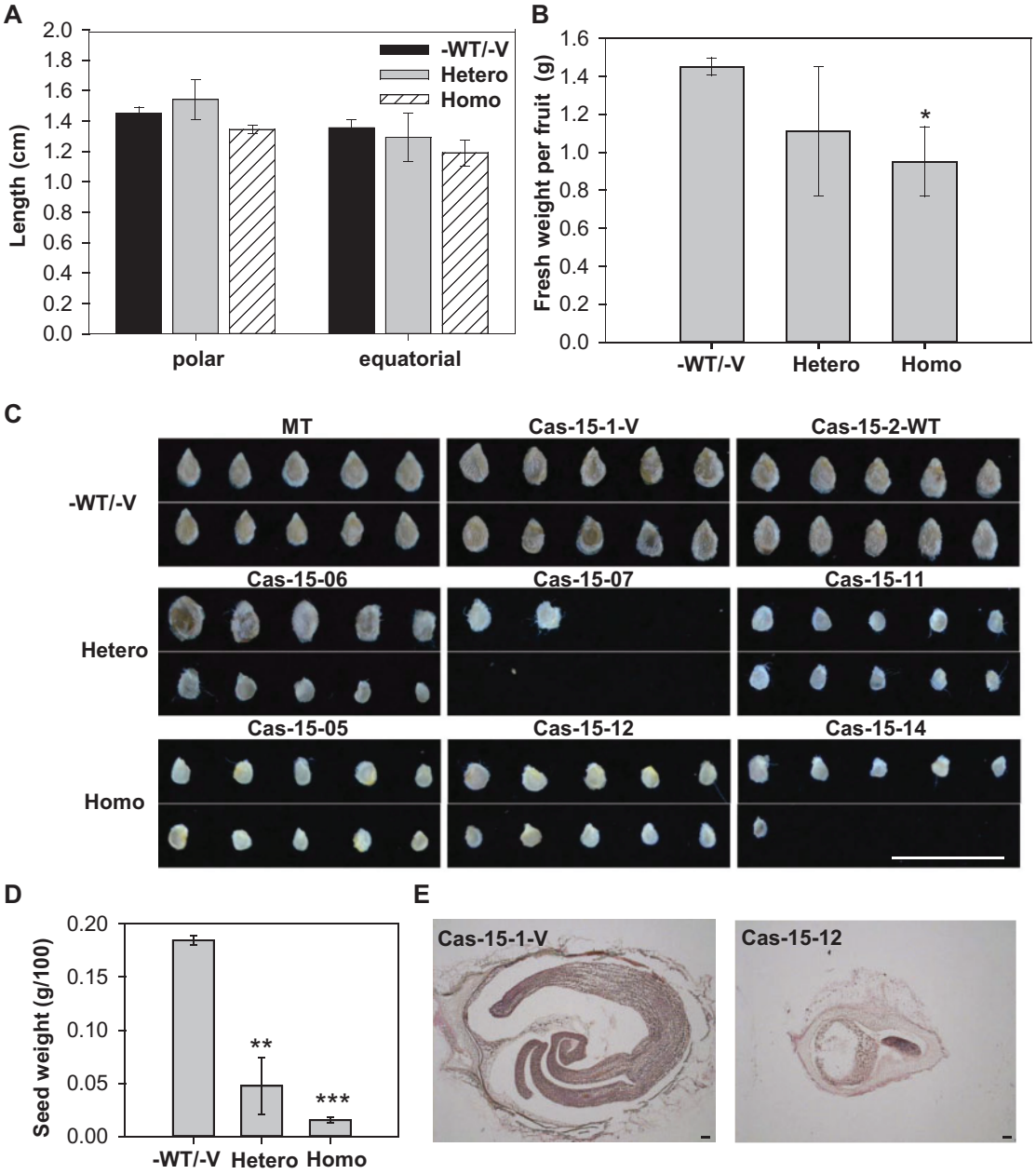

Figure 6 Fruit and seed development in *slsweet15* KO mutant plants. A and B, Fruit quality of T0 transgenic tomato plants. Mature red fruits were harvested and polar diameters, equatorial diameters (A) and fresh weights (B) were measured. C, Seeds of T0 transgenic tomato plants. Pictures are of representative seeds derived from WT MT, transgenic plants without mutation (Cas-15-1-V and Cas-15-2-WT), and Hetero, and Homo mutants. Bar = 1 cm. D, Seed weight of T0 transgenic tomato plants. E, Longitudinal sections of WT and mutant seed. Bar = 100 μm. WT, V indicated transgenic plants containing nonmutated genotype without or with the vector. Results are mean ± SE from averages of 3–4 transgenic lines. Differences from -WT/-V (Student's *t* test): $^{*}P < 0.05$, $^{**}P < 0.01$, or $^{***}P < 0.001$.

contents in pear fruits were closely linked with expression levels of PuSWEET15 (Li et al., 2020). These results highlighted a conserved sucrose transport feature of Clade III SWEET transporters in both seed and fruit crops. Based on high identities (up to 48%) to its close Arabidopsis putative ortholog AtSWEET12 (K_m ~70 mM, Supplemental Figure S7B; Chen et al., 2012), SlSWEET15 transporter probably also operated as a passive facilitator with low affinity, consistent with most characterized SWEET facilitators expressed in sink organs (Guo et al., 2014; Sosso et al., 2015; Ho et al., 2019). This passive transport feature fits well with proposed passive sucrose export from the phloem to the tomato pericarp (Ruan and Patrick, 1995; Lalonde et al., 2003). Moreover, high sucrose concentrations in SE-CCs, predicted to up to 500 mM and the steep concentration gradients (>100-fold) of sucrose across the plasma membrane (Damon et al., 1988; Ruan et al., 1996), would favor a low-affinity facilitator, like SlSWEET15. Based on accumulation of

transcripts and proteins in vascular cells, as well as localization on the plasma membrane, the passive sucrose-specific transport feature prompted us to propose that SlSWEET15 facilitated an energy-efficient sucrose-specific efflux from the plasma membrane of SE-CCs or VPCs to fruit apoplasm to support fruit expansion (Figure 7).

SlSWEET15 probably participates in intracellular sucrose homeostasis in fruit pericarps

Once sucrose is exported to the apoplasm of tomato pericarps, it has been estimated that 70% of apoplasmic sucrose is hydrolyzed by cell wall inverses as hexoses, which should be quickly taken up into surrounding SPCs by an energy coupled hexose/proton symporter to maintain a substantial sucrose concentration gradient for continuous unloading (Ruan and Patrick, 1995; Brown et al., 1997; McCurdy et al., 2010). Nevertheless, based on uptake of radioactive sucrose in pericarp, a small but significant portion of sucrose can be directly imported intact into fruit cytosols (Damon et al., 1988; Johnson et al., 1988; N'tchobo et al., 1999). The nonsaturated and PCMBS-insensitive characteristic of sucrose uptake into pericarp cells is consistent with an energy-independent sucrose transport mechanism, such as catalyzed by SlSWEET15 (Damon et al., 1988; Johnson et al., 1988; Brown et al., 1997). The passive sucrose fluxes are fully consistent with a low proton ATPase activity in pericarp cells (Johnson et al., 1988). Thus, it is likely that plasma membrane and tonoplast localized SlSWEET15 also facilitates sucrose import from the apoplasm to the cytosol and, subsequently, to the vacuole of SPCs for continuous intracellular sugar allocation (Figure 7). Conversely, once sucrose is uploaded into fruit cells, most sugars stored in fruit vacuoles are glucose or fructose (Gillaspy et al., 1993; Milne et al., 2018; Vu et al., 2020). Notwithstanding, these stored hexoses could be exported to the cytosol for metabolism and re-synthesis of sucrose, catalyzed by sucrose phosphate synthase (N'tchobo et al., 1999). Changes in cellular sugar signatures are constantly ongoing, especially during fruit maturation (N'tchobo et al., 1999) and a transient accumulation of sucrose in the cytosol of pericarp cells has been observed (Obiadalla-Ali et al., 2004). Based on increased accumulation of SlSWEET15 activity in pericarp cells during fruit maturation (Supplemental Figure S5), vacuole-targeted SlSWEET15 might thus provide an energy-independent strategy to regulate sucrose homeostasis between the cytosol and vacuole of fruit cells.

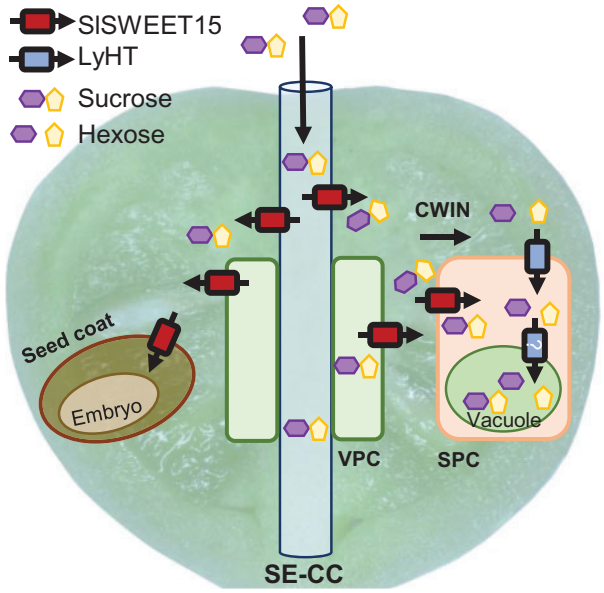

Figure 7 A functional model of SlSWEET15 during fruit and seed development. During fruit expansion in tomato, SlSWEET15 proteins gradually accumulate on plasma membrane of vascular bundles and neighboring parenchyma cells in fruit pericarp as well as seed coat. When sucrose is translocated from source leaves to developing tomato fruits, SlSWEET15 may facilitate sucrose unloading from the cytosol of SE-CC complexes or VPCs to the fruit apoplasm for sugar allocation. In addition, a portion of apoplasmic sucrose could be passively imported by the SlSWEET15 uniporter into SPCs. Conversely, sucrose is also hydrolyzed by cell wall invertase and imported by the active hexose transporter (LyHT). In seeds, SlSWEET15 also functions on the plasma membrane of seed coat cells to mediate sucrose importation into an embryo for seed filling.

SlSWEET15 may function in sucrose unloading from the seed coat

Pronounced accumulation of SlSWEET15 transcripts and proteins in seed coats, endosperm, and funiculus vascular cells implied that SlSWEET15 was also involved in sucrose unloading in tomato seeds, which have strong nutrient requirements and are enriched with transporter proteins (Pattison et al., 2015). Requirement of a SlSWEET15 transporter was consistent with a mandatory apoplasmic transport step between maternal (seed coat)-filial (endosperm or embryo) interface in tomato fruits (Ruan et al., 2012). Based on phloem-mobile fluorescent tracers or proteins, sucrose is apparently mostly unloaded from funiculus SE-CCs symplasmically to seed coats (Patrick and Offler, 2001; Zhang et al., 2007), which develop from the ovule integument (Quinet et al., 2019). These integument cells enclose the embryo and are the major site for nutrient release in most developing dicot seeds, as reported in Arabidopsis (Stadler et al., 2005) and legume seeds (Wang et al., 1995). Yet, there is a symplasmic disconnection between outer and inner integuments in Arabidopsis (Werner et al., 2011), or between seed coat parenchyma cells and filial storage sites in legume seeds (Wang et al., 1995). A similar apoplasmic barrier was reported in monocot wheat and rice grains (Oparka and Gates, 1981; Wang and Fisher, 1995). In this scenario, a plasma membrane carrier, such as SlSWEET15, would be required to mediate sucrose efflux to seed apoplasm. The proton-independent transport feature of the SWEET family is consistent with facilitated diffusion of sucrose efflux from seed coats (Zhang et al., 2007; Milne et al., 2018), as demonstrated in pea (De Jong et al., 1996; Zhou et al., 2007) and wheat (Wang and Fisher, 1995). The low-affinity transport feature of SWEET proteins can also be physiologically

favored, due to a substantial transmembrane sucrose concentration gradient (up to 50 mM) in maternal releasing cells in wheat grains and legume seeds (Fisher and Wang, 1995; Zhang et al., 2007). Based on these results, we inferred that SlSWEET15 probably facilitated sucrose unloading from funiculus phloem cells and sucrose efflux from the seed coat cells for seed filling (Figure 7).

SlSWEET15-mediated sucrose unloading was required for fruit and seed development

Genetic evidence from CRISPR/Cas9 KO tomato mutants confirmed the physiological role of SlSWEET15 in fruit development and seed filling (Figure 5). A lack of SlSWEET15 transport significantly reduced fruit growth and yield in Micro-Tom (MT) tomato (Figure 6, A and B), probably due to an inadequate sucrose supply from the releasing phloem. Similarly, seeds were mostly aborted or flaky and lacked embryo development (Figure 6, C–E). These phenotypes were consistent with the role of SWEET15 analogs in nonfruit plants. In Arabidopsis seeds, AtSWEET15, together with two Clade III SWEET, AtSWEET12 and 11, supported a cascade of sucrose transport from the outer and inner integuments to facilitate sucrose exchange from endosperm to embryo (Chen et al., 2015b). In rice seeds, OsSWEET15 collaborated with OsSWEET11 to mediate sucrose export from VPCs into the apoplsmic space, enabling allocation and also export from the nucellar epidermis/eleurone interface to support seed filling (Yang et al., 2018). Defects in SWEET-mediated sucrose transport caused wrinkled and undeveloped seeds (Chen et al., 2015b; Yang et al., 2018). Collectively, these studies supported a conserved function of Clade III SWEET in sucrose unloading for seed development. In fleshy fruit crops, the same SWEET15 transport system to participate in sucrose unloading in both seed and fruit cells may reflect a close association between seed and fruit development, where signals derived from developing seeds control the rate of cell division in surrounding fruit tissues (Gustafson, 1939; Gillaspy et al., 1993).

In summary, our current studies revealed a key role of *Sl*SWEET15 in sucrose unloading during fruit and seed development (Figure 7). We propose that in fast-growing green fruits, sucrose is largely allocated from source leaves to SE-CC complexes or surrounding VPCs in sink fruits. Due to symplasmic disconnection to fruit SPCs, plasma membrane-located SlSWEET15 expressed in SE-CCs/VPCs facilitates initial sucrose export from releasing phloem to fruit apoplasm. Then, a part of sucrose could be further imported into SPCs by SlSWEET15 expressed in nearby pericarp SPCs, especially during fruit maturation stage. The SlSWEET15-mediated sucrose unloading is also utilized during the apoplasmic sucrose transport in developing seeds, where SlSWEET15 located in the plasma membrane of seed coat promotes sucrose export to support carbon requirement for endosperm and embryo development in tomato seeds (Figure 7). Thus, increasing SlSWEET15 export activity by genetic engineering may provide a promising strategy to increase sucrose unloading for enhancement of fruit yield and quality in the future.

Materials and methods

Plant and growth conditions

Tomato (*Solanum lycopersicum*) MT was used in this study. Tomato seeds were sterilized using a bleach solution (30% v/v CLOROX and 0.1% v/v Triton X-100) for 8 min and then washed twice with sterilized water. Tomato seeds were germinated in water for 2–3 d and transferred to soil mixture directly or to 1/2 Murashige and Skoog (MS) liquid media (0.215% w/v MS medium, 0.1% w/v MES (2-(N-morpholino)ethanesulfonic acid), and 1.5% w/v Agar) for hydroponics cultivation. All plants were grown in a controlled chamber (25°C, 16-h/8-h light/dark, with ∼100 μmol m^{-2} s^{-1} illumination). To analyze gene expression, various organs, including roots, stems, young leaves (<2 cm long), and MLs (>4 cm, terminal leaflet) were collected from 4-week-old tomato plants grown hydroponically. Flower buds (3, 6 mm in length), flowers (1 DAA, 1 d after anthesis), fruits of 14 (immature green), 21 (mature green), 35 (breaker), and 42 (red) DAA were collected from 5- to 6-week-old plants. All organs were stored at −80°C before analysis.

RNA extraction

Fruit RNA transcripts were isolated according to the (1-Hexadecyl)trimethyl-ammonium bromide (CTAB) extraction method (Zhang et al., 2013). The extraction buffer contained 3% w/v CTAB, 1.4 M NaCl, 20 mM ethylenediaminetetraacetic acid (EDTA), 100 mM tris(hydroxymethyl)aminomethane (Tris)–HCl, 2% w/v Polyvinylpyrrolidone 40 (PVP40), and 2% v/v β-Mercaptoethanol (pH 8). In short, samples were ground into powder and mixed with preheated CTAB extraction buffer and incubated at 65°C for 30 min. After centrifugation (8,000*g* for 15 min), the supernatant was transferred to a new tube and mixed with an equal volume of chloroform:isoamylalcohol (24:1, v/v). The mixture was centrifuged (12,000*g* for 30 min) and the supernatant was transferred and mixed with 1/3 volume of 10 M LiCl. The reaction was incubated at −20°C overnight. Pellets were collected by centrifugation, washed twice with 200 μL 4 M LiCl, and suspended in 180 μL of 10 mM Tris–HCl (pH 7.5) and 20 μL of 3 M potassium acetate (pH 5.5). These mixtures were kept on ice for 30 min and then centrifuged. The supernatant was transferred and mixed with the 2.5 volume of pre-cold isopropyl alcohol and stored at −70°C for 3 h. The RNA pellets were collected by centrifugation and washed with 75% v/v ethanol and then dissolved in 20-μL DEPC water.

RNA samples from other organs (except for fruits) were isolated using TRIzol reagent as instructed (Thermo Fisher Scientific Inc., Waltham, MA, USA). In short, samples were ground into powders, mixed with 500-μL TRIzol reagent, and centrifuged. The mixtures were then transferred, mixed with 200-μL pre-cold chloroform:isoamyl alcohol (24:1, v/v) and centrifuged. The supernatant was added to 0.5 volume

of 99% v/v alcohol and resulting whole mixtures were transferred to an RNA spin column and processed as instructed (GeneMark, http://www.genemarkbio.com/). The RNA samples were suspended in 25-μL nuclease-free water and stored at −80°C until analyzed.

RT-qPCR analysis

Total RNA transcripts were reverse-transcribed and gene-specific primers for 30 *SlSWEET* genes were used for RT-qPCR, as described (Ho et al., 2019). To analyze expression in mutants, primers specific for full-length of *SlSWEET15* (5′-TOPO-SlSWT15-F and 3′-TOPO-SlSWT15-R, Supplemental Table S1) were used for PCR. The products were cloned into the vector pGM-T, as instructed (Genomics, Redwood City, CA, USA). For each line, 3–6 derived clones were sequenced. The reference gene *SlActin7* was used to determine relative expression.

In situ hybridization

To prepare the probe, partial *SlSWEET15* coding sequences of 246 bp were amplified with specific primers (RNAi-15-F and RNAi-15-R; Supplemental Table S1) and cloned into the vector pGM-T (pGM-T-RNAi-15; Genomics). Digoxigenin-labeled sense and antisense RNA probes were synthesized following manufacturer's instructions (Roche Applied Science, Penzberg, Germany). Mature green fruits (21 DAA) were sliced and fixed in pH 7.0 PFA solution (4% w/v paraformaldehyde, 35-mM sodium hydroxide, 0.1% v/v tween 20 and 0.1% v/v Triton X-100 in 250 mL phosphate-buffered saline for 16 h at 4°C. Samples were then dehydrated through an ethanol series and embedded into molten wax (Leica, Wetzlar, Germany). Thick (10 μm) sections were cut on a MICROM 315R microtome (Thermo Scientific, Waltham, MA, USA). Hybridization and immunological detection of fluorescent signals were detected with anti-digoxigenin-POD (Roche) and using the TSA™ PLUS FLUORESCENCE SYSTEMS according to manufacturer's instructions (PerkinElmer, Waltham, MA, USA). To identify SEs, the consecutive sections were incubated in 0.05% w/v aniline blue (dissolved in 67-mM phosphate buffer, pH 8.5) for 5 min following with two washes (Ruan et al., 2004) and fluorescence was examined. All fluorescent signals of sections were observed on a ZEISS LSM 710 confocal microscope. The Opal670 fluorescence was visualized by excitation with a 633-nm laser (6%–9%) and emission between 633 and 670 nm (master gain = 180–200, digital gain = 1.10), whereas aniline blue fluorescence was visualized by excitation with a 405 nm laser (2.2%) and emission between 415 and 730 nm (master gain = 200, digital gain = 1.10). Alternative detection with alkaline phosphatase was also done as described (Lin et al., 2014). All the detections were performed by RNA ISH Core Facility of Academia Sinica.

Expression of GUS fusions

The *SlSWEET15* (Solyc09g074530) promoter (2,000-bp upstream to ATG) and genomic opening reading frame, including all introns (1,348 bp after ATG) were amplified from genomic DNA with specific primers (SWT15-promoter-F and SWT15-promoter-R for promoter and SWT15-g-F and SWT15-g-R for open reading frame; Supplemental Table S1). The SlSWEET15 promoter fragments were purified and cloned into the binary vector pUTKan by SacI and SacII sites (pUTKan-$P_{SWEET15}$). The SlSWEET15 genomic ORF was then cloned into pUTKan-$P_{SWEET15}$ via SacII and BamHI sites. Tomato plants were transformed with the resulting pUTKan-$P_{SWEET15}$::gSlSWEET15 binary vector in the Transgenic Plant Core Lab in Academia Sinica (http://transplant.sinica.edu.tw/en/-aboutus/intro/index3.htm) and three positive T0 transgenic tomato plants were obtained. Mature fruits of two T0 transgenic plants and various organs from Hetero soil-grown T1 plants were collected and histochemically stained for 16 h, as described (Ho et al., 2019).

Confocal microscopy for GFP fusions

To observe subcellular localization in planta, the *SlSWEET15* cDNA fragment without the stop codon was amplified with a specific primer (5′-UTR-SlSWT15 and attb-dTGA-R SWT15; Supplemental Table S1), then cloned into the pDONR221 (pDONR221f1-SWT15-dTGA). The *SlSWEET15* cDNA was then transferred from the pDONR221 clone into p2GWF7 (Karimi et al., 2007). Arabidopsis (*A. thaliana*) protoplasts were isolated and transfected with resultant vector p2GWF7-SWT15, as described (Wu et al., 2009). To localize the position of inner membranes, plasma membrane marker AtPIP2A:RFP fusions (Nelson et al., 2007), or the vacuolar membrane protein AtrTIP:RFP fusion (Jauh et al., 1999) were also expressed with SlSWEET15-GFP in protoplasts. After 20–34 h of transformation, fluorescence imaging of protoplasts was performed. To observe localization in vacuoles, Arabidopsis protoplasts were lysed by addition of so-called lysis buffer medium (10 mM 4-(2-hydroxyethyl)-1-piperazineethanesulfonic acid, 20 mM EDTA pH 8 and 200 mM sorbitol) for at least 15 min before observation.

For transient expression in *N. benthamiana* leaves, the fragment (3,094 bp) including CaMV35s promoter-SWT15-GFP-CaMV terminator was amplified from p2GWF7 to SWT15 with specific primer (35S-F and CaMVTer-R, Supplemental Table S1) and then cloned into pJH212 binary vector by BamHI and HindIII restriction sites. The resulted binary vector pJH212-SWT15-GFP was then transferred into *Agrobacterium tumefaciens* (GV3101 strain). The *N. benthamiana* leaf infiltration was performed as described previously (Sosso et al., 2015). All images of GFP fluorescence were done on a Carl Zeiss LSM780 confocal microscope (Instrument Development Center, NCKU). The GFP fluorescence was visualized by excitation with an Argon Laser at 488 nm (50% for protoplasts and 7.5% for leaf cells) and emission between 500 and 545 nm (master gain = 780–800, digital gain = 1), whereas RFP fluorescence was visualized by excitation with a 561 nm laser (1.8%) and emission between 566 and 585 nm (master gain = 700–780, digital gain = 1).

Complementation assays in yeast (*S. cerevisiae*)

To express SlSWEET15 in yeast, cDNA sequence (861 bp) was amplified using Phusion polymerase (New England Biolabs, Ipswich, MA, USA) with gene-specific primers (attb-SlSWT15-F and attb-SlSWT15-R). The cDNA was first cloned into the pDONR221-f1 vector (pDONR221f1-SWT15) using BP cloning and subsequently transferred to the pDRf1-GW vector (pDRf1-GW-SWT15) using LR Gateway technology (Grefen et al. 2010). To express SlSWEET15-GFP in yeast, the SlSWEET15 cDNA was transferred from the pDONR221f1-SWT15-dTGA into pDRGW-eGFP (pDRGW-SWT15-eGFP; Chen et al. 2015a). The yeast strain YSL2-1 was transformed with the resulting constructs using the lithium acetate method (Chen et al. 2015a). For growth assay, transformants were selected and spotted on synthetic deficient media supplemented with or without various concentrations of sugars as described previously (Ho et al. 2019). GFP fluorescence in log-phase yeast cells was observed on a Carl Zeiss LSM780 confocal microscope. The GFP fluorescence was visualized by excitation with an Argon Laser at 488 nm (30%) and emission between 500 and 545 nm (master gain = 750, digital gain = 1). Sequences of primers are provided in Supplemental Table S1.

Creating a SlSWEET15 mutant line using CRISPR/Cas9

To create fragment deletion of *SlSWEET15*, two targeted sequences (T1 and T2), from positions +266 and +323 downstream of the translation start site (ATG), were chosen according to a website (https://crispr.cos.uni-heidelberg.de/; Figure 5A). Targeted sequences were synthesized and the whole gRNA scaffold including T1 and T2 sequences were amplified with specific primers (DT1-SlSWT15-F0 and DT2-SlSWT15-R0) using the module vector pCBC-DT1T2 as a template. Resulting RNA scaffold products were used in an overlap PCR reaction with specific primers (SlSWT15-DT1-BsF and SlSWT15-DT2-BsR; Brooks et al., 2014). Thereafter, resulting PCR products containing the pCBC-DT1T2 *SlSWEET15*-specific cassette were digested with BsaI and inserted into the binary vector pKSE401 (Brooks et al., 2014), which was then introduced into an Agrobacterium strain and transformed into MT tomato plant by the Transgenic Plant Core Lab in Academia Sinica (http://transplant.sinica.edu.tw/en/aboutus/intro/index3.htm). Nineteen positive T0 transgenic tomato plants were regenerated, transferred to soils, and grown and fruits and seeds were collected. All primer sequences are shown in Supplemental Table S1.

Genomic DNA extraction and PCR analysis

A mature leaf was collected from each T0 transgenic tomato plant and stored at −80°C pending analysis. Leaf samples were placed in liquid nitrogen, ground into powder and mixed with 500 µL CTAB extraction buffer (3% w/v CTAB, 1.4 M sodium chloride, 2% w/v PVP40, 20 mM pH8 EDTA and 100 mM pH8 Tris–HCl). Mixtures were incubated at 55°C for 15 min and centrifuged at 12,000*g* for 5 min. The supernatant was transferred to new tubes, 250-µL chloroform:isoamyl alcohol (24:1, v/v) was added and the solution was vortexed and then centrifuged at 13,000*g* for 1 min. The upper supernatant was removed and placed in 37.5 µL of 10 M ammonium acetate and 500 µL of pre-cold 99% v/v alcohol and kept at −20°C for 2–3 h, then centrifuged at 13,000*g* for 1 min. Resulting pellets were washed twice with 70% v/v alcohol, incubated at 60°C for 5 min and finally re-suspended in 20 µL of nuclease-free water. To confirm mutation types in transgenic tomato plants, partial *SlSWEET15* fragments were amplified from genomic DNA with specific primers (P1 and P2) and cloned into the vector pGM-T, as instructed (Genomics, Taipei, Taiwan). For each line, 3–6 derived clones were sequenced. To examine the transformation event, the gene sequence of Cas9 gene was also amplified with specific primers (Cas9-F and Cas9-R). All primer sequences are listed (Supplemental Table S1).

Phylogenetic analysis

Amino acid sequences of *SWEET* genes from various species and tomato were downloaded from NCBI GenBank (https://www.ncbi.nlm.nih.gov/gene/) and Sol Genomics Net (https://solgenomics.net/), respectively. These sequences were then aligned using Clustal Omega (https://www.ebi.ac.uk/ Tools/msa/clustalo/). The phylogenetic tree was then generated using MEGA (https://www.megasoftware.net/).

Accession numbers

Accession numbers of major genes mentioned in this study are shown in Supplemental Figure S7.

Supplemental data

The following materials are available in the online version of this article.

Supplemental Table S1. The list of primers used in this study

Supplemental Table S2. Phenotypes of fruit and seed production in CRISPR-Cas9-induced SlSWEET15 mutation in T0 transgenic tomato plants

Supplemental Figure S1. Expression of *SlSWEETs* in developing tomato fruits.

Supplemental Figure S2. Sequence alignment of type III *SlSWEET* genes.

Supplemental Figure S3. Tissue-specific localization of *SlSWEET15* in tomato fruits.

Supplemental Figure S4. Localization of *SlSWEET15* transcripts in unloading cells of tomato fruits.

Supplemental Figure S5. Accumulation of SlSWEET15 proteins during fruit maturation in tomato.

Supplemental Figure S6. Localization of SlSWEET15 on the tonoplast during lysis.

Supplemental Figure S7. Phylogenetic comparison of type III *SWEET* genes.

Supplemental Figure S8. Transport activities of SlSWEET15 to hexoses in yeast.

Supplemental Figure S9. Characterizations of Cas9-mediated mutant plants.

Acknowledgments

We thank Ruth Wartenberg and Chein Wein Yu to assist transient expression in Arabidopsis. We also thank the RNA ISH Core Facility of Academia Sinica for performing the ISH experiment. Finally, we are very grateful for constructive comments provided by Dr. Peter Goldsbrough in Purdue University (IN, USA).

Funding

This work was financially supported by grants from the Ministry of Science and Technology, Taiwan (MOST 105-2628-B-006-001-MY3; MOST 108-2314-B-006-077-MY3) to W.J.G. Work in the lab of H.E.N was supported by the Deutsche Akademische Austauschdienst (DAAD Project-Based Personal Exchange Program Germany 106-2911-I-006-506).

Conflict of interest statement. The authors have no conflict of interest to declare.

References

Ariizumi T, Higuchi K, Arakaki S, Sano T, Asamizu E, Ezura H (2011) Genetic suppression analysis in novel vacuolar processing enzymes reveals their roles in controlling sugar accumulation in tomato fruits. J Exp Bot **62**: 2773–2786

Barker L, Kühn C, Weise A, Schulz A, Gebhardt C, Hirner B, Hellmann H, Schulze W, Ward JM, Frommer WB (2000) SUT2, a putative sucrose sensor in sieve elements. Plant Cell **12**: 1153–1164

Baxter CJ, Carrari F, Bauke A, Overy S, Hill SA, Quick PW, Fernie AR, Sweetlove LJ (2005) Fruit carbohydrate metabolism in an introgression line of tomato with increased fruit soluble solids. Plant Cell Physiol **46**: 425–437

Bezrutczyk M, Hartwig T, Horschman M, Char SN, Yang J, Yang B, Frommer WB, Sosso D (2018) Impaired phloem loading in *zmsweet13a,b,c* sucrose transporter triple knock-out mutants in *Zea mays*. New Phytol **218**: 594–603

Braun DM, Wang L, Ruan YL (2014) Understanding and manipulating sucrose phloem loading, unloading, metabolism, and signalling to enhance crop yield and food security. J Exp Bot **65**: 1713–1735

Brooks C, Nekrasov V, Lippman ZB, Van Eck J (2014) Efficient gene editing in tomato in the first generation using the clustered regularly interspaced short palindromic repeats/CRISPR-associated9 System. Plant Physiol **166**: 1292–1297

Brown MM, Hall JL, Ho LC (1997) Sugar uptake by protoplasts isolated from tomato fruit tissues during various stages of fruit growth. Physiol Plant **101**: 533–539

Carpaneto A, Koepsell H, Bamberg E, Hedrich R, Geiger D (2010) Sucrose- and H-dependent charge movements associated with the gating of sucrose transporter ZmSUT1. PLoS One **5**: e12605

Chen HY, Huh JH, Yu YC, Ho LH, Chen LQ, Tholl D, Frommer WB, Guo WJ (2015a) The Arabidopsis vacuolar sugar transporter SWEET2 limits carbon sequestration from roots and restricts *Pythium* infection. Plant J **83**: 1046–1058

Chen LQ (2013) SWEET sugar transporters for phloem transport and pathogen nutrition. New Phytol **201**: 1150–1155

Chen LQ, Lin IW, Qu XQ, Sosso D, McFarlane HE, London~o A, Samuels AL, Frommer WB (2015b) A cascade of sequentially expressed sucrose transporters in the seed coat and endosperm provides nutrition for the arabidopsis embryo. Plant Cell Online **27**: 607–619

Chen LQ, Qu XQ, Hou BH, Sosso D, Osorio S, Fernie AR, Frommer WB (2012) Sucrose efflux mediated by SWEET proteins as a key step for phloem transport. Science **335**: 207–211

Chen LQ, Hou BH, Lalonde S, Takanaga H, Hartung ML, Qu XQ, Guo WJ, Kim JG, Underwood W, Chaudhuri B, et al. (2010) Sugar transporters for intercellular exchange and nutrition of pathogens. Nature **468**: 527–532

Cohn M, Bart RS, Shybut M, Dahlbeck D, Gomez M, Morbitzer R, Hou BH, Frommer WB, Lahaye T, Staskawicz BJ (2014) *Xanthomonas axonopodis* virulence is promoted by a transcription activator-like effector–mediated induction of a SWEET sugar transporter in Cassava. Mol Plant Microbe Interact **27**: 1186–1198

Cox KL, Meng F, Wilkins KE, Li F, Wang P, Booher NJ, Carpenter SCD, Chen LQ, Zheng H, Gao X, et al. (2017) TAL effector driven induction of a SWEET gene confers susceptibility to bacterial blight of cotton. Nat Commun **8**: 15588

Czerednik A, Busscher M, Bielen BAM, Wolters-Arts M, de Maagd RA, Angenent GC (2012) Regulation of tomato fruit pericarp development by an interplay between CDKB and CDKA1 cell cycle genes. J Exp Bot **63**: 2605–2617

Damon S, Hewitt J, Nieder M, Bennett AB (1988) Sink metabolism in tomato fruit: II. Phloem unloading and sugar uptake. Plant Physiol **87**: 731–736

De Jong A, Koerselman-Kooij JW, Schuurmans JAMJ, Borstlap AC (1996) Characterization of the uptake of sucrose and glucose by isolated seed coat halves of developing pea seeds. Evidence that a sugar facilitator with diffusional kinetics is involved in seed coat unloading. Planta **199**: 486–492

Eom JS, Chen LQ, Sosso D, Julius BT, Lin IW, Qu XQ, Braun DM, Frommer WB (2015) SWEETs, transporters for intracellular and intercellular sugar translocation. Curr Opin Plant Biol **25**: 53–62

Feng CY, Han JX, Han XX, Jiang J (2015) Genome-wide identification, phylogeny, and expression analysis of the SWEET gene family in tomato. Gene **573**: 261–272

Fisher DB, Wang N (1995) Sucrose concentration gradients along the post-phloem transport pathway in the maternal tissues of developing wheat grains. Plant Physiol **109**: 587–592

Gao Y, Zhang C, Han X, Wang ZY, Ma L, Yuan DP, Wu JN, Zhu XF, Liu JM, Li DP, et al. (2018) Inhibition of OsSWEET11 function in mesophyll cells improves resistance of rice to sheath blight disease. Mol Plant Pathol **19**: 2149–2161

Gillaspy G, Ben-David H, Gruissem W (1993) Fruits: a developmental perspective. Plant Cell **5**: 1439–1451

Grefen C, Donald N, Hashimoto K, Kudla J, Schumacher K, Blatt MR (2010) A ubiquitin-10 promoter-based vector set for fluorescent protein tagging facilitates temporal stability and native protein distribution in transient and stable expression studies. Plant J **64**: 355–365

Guo WJ, Nagy R, Chen HY, Pfrunder S, Yu YC, Santelia D, Frommer WB, Martinoia E (2014) SWEET17, a facilitative transporter, mediates fructose transport across the tonoplast of Arabidopsis roots and leaves. Plant Physiol **164**: 777–789

Gustafson FG (1939) Auxin distribution in fruits and its significance in fruit development. Am J Bot **26**: 189–194

Hackel A, Schauer N, Carrari F, Fernie AR, Grimm B, Kühn C (2006) Sucrose transporter LeSUT1 and LeSUT2 inhibition affects tomato fruit development in different ways. Plant J **45**: 180–192

Hetherington SE, Smillie RM, Davies WJ (1998) Photosynthetic activities of vegetative and fruiting tissues of tomato. J Exp Bot **49**: 1173–1181

Ho LH, Klemens PAW, Neuhaus HE, Hsieh SY, Ko HY, Guo WJ (2019) SlSWEET1a is involved in glucose import to young leaves in tomato plants. J Exp Bot **70**: 3241–3254

Ho LH, Lee YI, Hsieh SY, Lin IS, Wu YC, Ko HY, Klemens PA, Neuhaus HE, Chen YM, Huang TP, et al. (2021) GeSUT4 mediates sucrose import at the symbiotic interface for carbon

allocation of heterotrophic *Gastrodia elata* (orchidaceae). Plant Cell Environ **44**: 20–33

Hu L, Sun H, Li R, Zhang L, Wang S, Sui X, Zhang Z (2011) Phloem unloading follows an extensive apoplasmic pathway in cucumber (*Cucumis sativus* L.) fruit from anthesis to marketable maturing stage. Plant Cell Environ **34**: 1835–1848

Jauh GY, Phillips TE, Rogers JC (1999) Tonoplast intrinsic protein isoforms as markers for vacuolar functions. Plant Cell **11**: 1867–1882

Jin Y, Ni DA, Ruan YL (2009) Posttranslational elevation of cell wall invertase activity by silencing its inhibitor in tomato delays leaf senescence and increases seed weight and fruit hexose level. Plant Cell **21**: 2072–2089

Johnson C, Hall JL, Ho LC (1988) Pathways of uptake and accumulation of sugars in tomato fruit. Ann Bot **61**: 593–603

Karimi M, Depicker A, Hilson P (2007) Recombinational cloning with plant gateway vectors. Plant Physiol **145**: 1144–1154

Kuhn C, Grof CPL (2010) Sucrose transporters of higher plants. Curr Opin Plant Biol **13**: 287–297

Lalonde S, Tegeder M, Throne-Holst M, Frommer WB, Patrick JW (2003) Phloem loading and unloading of sugars and amino acids. Plant Cell Environ **26**: 37–56

Lemaire-Chamley M, Mounet F, Deborde C, Maucourt M, Jacob D, Moing A (2019) NMR-based tissular and developmental metabolomics of tomato fruit. Metabolites **9**: 93

Li X, Guo W, Li J, Yue P, Bu H, Jiang J, Liu W, Xu Y, Yuan H, Li T, Wang A (2020) Histone acetylation at the promoter for the transcription factor PuWRKY31 affects sucrose accumulation in pear fruit. Plant Physiol **182**: 2035–2046

Marques WL, Mans R, Marella ER, Cordeiro RL, van den Broek M, Daran J-MG, Pronk JT, Gombert AK, van Maris AJA (2017) Elimination of sucrose transport and hydrolysis in *Saccharomyces cerevisiae*: A platform strain for engineering sucrose metabolism. FEMS Yeast Research **17**: fox006

McCurdy DW, Dibley SJ, Cahyanegara R, Martin A, Patrick JW (2010) Functional characterization and RNAi-mediated suppression reveals roles for hexose transporters in sugar accumulation by tomato fruit. Mol Plant **3**: 1049–1063

Milne RJ, Grof CPL, Patrick JW (2018) Mechanisms of phloem unloading: shaped by cellular pathways, their conductances and sink function. Curr Opin Plant Biol **43**: 8–15

N'tchobo H, Dali N, Nguyen-Quoc B, Foyer CH, Yelle S (1999) Starch synthesis in tomato remains constant throughout fruit development and is dependent on sucrose supply and sucrose synthase activity. J Exp Bot **50**: 1457–1463

Nelson BK, Cai X, Nebenführ A (2007) A multicolored set of *in vivo* organelle markers for co-localization studies in Arabidopsis and other plants. Plant J **51**: 1126–1136

Obiadalla-Ali H, Fernie AR, Kossmann J, Lloyd JR (2004) Developmental analysis of carbohydrate metabolism in tomato (*Lycopersicon esculentum* cv. Micro-Tom) fruits. Physiol Plant **120**: 196–204

Oparka KJ, Gates P (1981) Transport of assimilates in the developing caryopsis of rice (*Oryza sativa* L.): The pathways of water and assimilated carbon. Planta **152**: 388–396

Osorio S, Ruan YL, Fernie AR (2014) An update on source-to-sink carbon partitioning in tomato. Front Plant Sci **5**: 516

Patrick JW (1997) Phloem unloading: sieve element unloading and post-sieve element transport. Annu Rev Plant Physiol Plant Mol Biol **48**: 191–222

Patrick JW, Offler CE (1996) Post-sieve element transport of photoassimilates in sink regions. J Exp Bot **47**: 1165–1177

Patrick JW, Offler CE (2001) Compartmentation of transport and transfer events in developing seeds. J Exp Bot **52**: 551–564

Pattison RJ, Csukasi F, Zheng Y, Fei Z, van der Knaap E, Catalá C (2015) Comprehensive tissue-specific transcriptome analysis reveals distinct regulatory programs during early tomato fruit development. Plant Physiol **168**: 1684–1701

Paul MJ, Nuccio ML, Basu SS (2018) Are GM crops for yield and resilience possible? Trends Plant Sci **23**: 10–16

Pesaresi P, Mizzotti C, Colombo M, Masiero S (2014) Genetic regulation and structural changes during tomato fruit development and ripening. Front Plant Sci **5**: 124

Quinet M, Angosto T, Yuste-Lisbona FJ, Blanchard-Gros R, Bigot S, Martinez J-P, Lutts S (2019) Tomato fruit development and metabolism. Front Plant Sci **10**: 1554

Ruan Yl, Patrick J (1995) The cellular pathway of postphloem sugar transport in developing tomato fruit. Planta **196**: 434–444

Ruan YL, Patrick JW, Bouzayen M, Osorio S, Fernie AR (2012) Molecular regulation of seed and fruit set. Trends Plant Sci **17**: 656–665

Ruan YL, Patrick JW, Brady CJ (1996) The composition of apoplastic fluid recovered from intact developing tomato fruit. Aust J Plant Physiol **23**: 9–13

Ruan YL, Xu SM, White R, Furbank RT (2004) Genotypic and developmental evidence for the role of plasmodesmatal regulation in cotton fiber elongation mediated by callose turnover. Plant Physiol **136**: 4104–4113

Schulze W, Weise A, Frommer WB, Ward JM (2000) Function of the cytosolic N-terminus of sucrose transporter AtSUT2 in substrate affinity. FEBS Lett **485**: 189–194

Shammai A, Petreikov M, Yeselson Y, Faigenboim A, Moy-Komemi M, Cohen S, Cohen D, Besaulov E, Efrati A, Houminer N, et al. (2018) Natural genetic variation for expression of a SWEET transporter among wild species of *Solanum lycopersicum* (tomato) determines the hexose composition of ripening tomato fruit. Plant J **96**: 343–357

Sosso D, Luo D, Li QB, Sasse J, Yang J, Gendrot G, Suzuki M, Koch KE, McCarty DR, Chourey PS, et al. (2015) Seed filling in domesticated maize and rice depends on SWEET-mediated hexose transport. Nat Genet **47**: 1489

Speth EB, Imboden L, Hauck P, He SY. (2009) Subcellular localization and functional analysis of the Arabidopsis GTPase RabE. Plant Physiol **149**: 1824–1837

Stadler R, Lauterbach C, Sauer N (2005) Cell-to-Cell movement of green fluorescent protein reveals post-phloem transport in the outer integument and identifies symplastic domains in arabidopsis seeds and embryos. Plant Physiol **139**: 701–712

Tao Y, Cheung LS, Li S, Eom JS, Chen LQ, Xu Y, Perry K, Frommer WB, Feng L (2015) Structure of a eukaryotic SWEET transporter in a homotrimeric complex. Nature **527**: 259–263

Vu DP, Martins Rodrigues C, Jung B, Meissner G, Klemens PAW, Holtgräwe D, Fürtauer L, Nägele T, Nieberl P, et al. (2020) Vacuolar sucrose homeostasis is critical for plant development, seed properties, and night-time survival in Arabidopsis. J Exp Bot **71**: 4930–4943

Walker AJ, Ho LC (1977) Carbon translocation in the tomato: carbon import and fruit growth. Ann Bot **41**: 813–823

Wang LF, Qi XX, Huang XS, Xu LL, Jin C, Wu J, Zhang SL (2016) Overexpression of sucrose transporter gene *PbSUT2* from *Pyrus bretschneideri*, enhances sucrose content in *Solanum lycopersicum* fruit. Plant Physiol Biochem **105**: 150–161

Wang N, Fisher DB (1995) Sucrose release into the endosperm cavity of wheat grains apparently occurs by facilitated diffusion across the nucellar cell membranes. Plant Physiol **109**: 579–585

Wang S, Yokosho K, Guo R, Whelan J, Ruan Y-L, Ma JF, Shou H (2019a) The soybean sugar transporter GmSWEET15 mediates sucrose export from endosperm to early embryo. Plant Physiol **180**: 2133–2141

Wang T, Zhang H, Zhu H (2019b) CRISPR technology is revolutionizing the improvement of tomato and other fruit crops. Hortic Res **6**: 77

Wang XD, Harrington G, Patrick JW, Offler CE, Fieuw S (1995) Cellular pathway of photosynthate transport in coats of developing seed of *Vicia faba* L. and *Phaseolus vulgaris* L. II. Principal cellular site(s) of efflux. J Exp Bot **46**: 49–63

Wang ZP, Deloire A, Carbonneau A, Federspiel B, Lopez F (2003) An *in vivo* experimental system to study sugar phloem unloading in ripening grape berries during water deficiency stress. Ann Bot **92**: 523–528

Werner D, Gerlitz N, Stadler R (2011) A dual switch in phloem unloading during ovule development in Arabidopsis. Protoplasma **248**: 225–235

Wu FH, Shen SC, Lee LY, Lee SH, Chan MT, Lin CS (2009) Tape-Arabidopsis Sandwich - a simpler Arabidopsis protoplast isolation method. Plant Methods **5**: 16

Yang J, Luo D, Yang B, Frommer WB, Eom JS (2018) SWEET11 and 15 as key players in seed filling in rice. New Phytol **218**: 604–615

Zhang LY, Peng YB, Pelleschi-Travier S, Fan Y, Lu YF, Lu YM, Gao XP, Shen YY, Delrot S, Zhang DP (2004) Evidence for apoplasmic phloem unloading in developing apple fruit. Plant Physiol **135**: 574–586

Zhang L, Zhang Z, Lin S, Zheng T, Yang X (2013) Evaluation of six methods for extraction of total RNA from Loquat. Not Bot Horti Agrobo **41**: 313–316

Zhang WH, Zhou Y, Dibley KE, Tyerman SD, Furbank RT, Patrick JW (2007) Nutrient loading of developing seeds. Funct Plant Biol **34**: 314–331

Zhou Y, Qu H, Dibley KE, Offler CE, Patrick JW (2007) A suite of sucrose transporters expressed in coats of developing legume seeds includes novel pH-independent facilitators. Plant J **49**: 750–764